Chemical Physics 531 (2020) 110662

Contents lists available at ScienceDirect

Chemical Physics

journal homepage: www.elsevier.com/locate/chemphys

Design of polymer membrane morphology with prescribed structure and diffusion properties

Anna Strzelewicz[a,*], Monika Krasowska[a], Gabriela Dudek[a], Michał Cieśla[b]

[a] Department of Physical Chemistry and Technology of Polymers, Faculty of Chemistry, Silesian University of Technology, Strzody 9, 44-100 Gliwice, Poland
[b] M. Smoluchowski Institute of Physics, Jagiellonian University, Łojasiewicza 11, 30–348 Kraków, Poland

ARTICLE INFO

Keywords:
Membrane modelling
Simulation
Morphological analysis
Structure-properties relationship

ABSTRACT

We study the possibility of using numerical modelling in the process of design a membrane of prescribed morphology and transport properties. We started from a real example of the cross-section of alginate membrane cross-linked by glutaraldehyde containing 25 wt% magnetite particles and searched for a numerical model that will resemble its morphological properties like amount of polymer matrix, sizes of polymer matrix domains, fractal dimension and others. Two different methods of generating models of such were proposed. After choosing the best models based on its morphological similarities to the real membrane, we study their transport properties in terms of Brownian diffusion. We showed that there is a good agreement of diffusion type and diffusion constant between the models and the real membrane.

1. Introduction

The search for new materials and the improvement of the existing ones in membrane technology is a difficult and complex subject, especially, if transport and structure-morphology problems have to be taken into account [1–4]. These properties are not only important from the technological and utilitarian point of view but they may influence on a number of processes in a biological systems, as natural membranes plays there crucial role [5,6].

The increasing demand for improved membranes and applications has provoked the necessity for mass transport simulation methods, ensuring consideration of the interactions between different components of the system and the influence of process parameters on the permeation fluxes [3,7]. The development of numerical algorithms can be very supportive in these studies. Computer-aided methods have proven useful in various scientific fields because they quickly screen a large amount of materials and structures in order to select optimal conditions, reagents, etc. for further research. The main benefit of such an approach is the optimization of the investigation process in order to run as few experiments as possible. The membrane structure is an element which can be influenced, i.e. created or modified, and its analysis is essential for proper material design in a variety of different applications [8].

If the polymers which form the membrane are qualitatively similar with respect to selectivity then they may be modified by various substitutions, insertion of metal cations, production of copolymers or incorporation of inorganic materials into the polymer matrix. After addition of some fillers, the membrane can be considered as a composite system. This system in membrane technology consists of at least two distinct and well-defined domains i which are characterized by different values of gas or vapour permeability P_i. The permeability of the total heterogeneous medium is related to P_i values, the volume fractions v_i of the component phases as well as to the system morphology, especially the shape and geometrical arrangement of each domain i [9–12]. An example of a heterogeneous membrane is a mixed matrix membrane, which consists of inorganic fillers i.e. magnetic powder embedded in a polymer matrix [13–15]. The aforementioned membranes are very effective in the separation of gases and vapors because they combine advantageous properties of both the polymer matrix and filler particles. The incorporation of fillers in the polymer matrix generally improves permeability or selectivity, or both, in comparison with a polymeric membrane.

Studies of such hybrid membranes have been undertaken with the purpose to enrich the air with oxygen or dehydration of ethanol in pervaporation [13,14]. It was observed that the enrichment of the air with oxygen rises with the increase of the magnetic powder amount [13] and improves the dehydration of ethanol [14]. Recently, the structure of the mentioned membranes has been detected as self-similar and the concept of fractals has been applied [16–18]. The fractal dimension and its generalizations are selected as a tool when considering

* Corresponding author.
E-mail address: astrzelewicz@polsl.pl (A. Strzelewicz).

https://doi.org/10.1016/j.chemphys.2019.110662
Received 9 December 2019; Accepted 17 December 2019
Available online 26 December 2019

mass transport through membranes and during the membrane casting process [19].

Fractal models may be used in studies of both static and dynamic properties, i.e. static fractal dimension d_f and fractal dimension of the trajectory of the random walk d_w. The motion of the particle, which could be a gas (vapor) particle diffusing in the membrane, is examined in Ref. [17]. The study employed numerical simulations, and suggested that the character of diffusion depends on texture, shape and size of the formed domains of magnetic powder in the membrane matrix, however, the overall conclusion is derived using a very limited number of membranes. To overcome this issue one need a large set of membranes with similar properties, which can be further tested numerically. Therefore, in this paper, the attention is focused on the computer-aided generation of prototype membrane structures, which resemble real structures.

The aim of this study is to check if it is possible to develop a numerical method of generating random membranes of the same morphological properties like a given real membrane in terms of observed amount of polymer matrix, fractal dimension, degree of multifractality, etc. Additionally, it is interesting to check, if such numerically generated objects have similar transport properties in terms of Brownian diffusion like the real one. In the case of positive result, such procedure can be used for numerical design of a membrane of the desired transport properties and then producing the real one basing only on morphological properties. This may significantly reduce costs of membrane design and production.

The paper is organized as follows: Sections 2 and 3 examine the structure of real and model membranes and a description of their structural parameters. Section 3.1 describes two example approaches to generate random structures resembling studied membranes. Fractal analysis and diffusion modelling is described in Sections 4.1 and 4.2, respectively. Section 5 discusses the obtained results. The paper ends with a short summary and conclusion.

2. Structure of a real membrane

The exemplary morphology of real hybrid membrane is shown in Fig. 1. The figure shows the cross-section of alginate membrane cross-linked by glutaraldehyde (AlgGA) containing 25wt% magnetite particles (Fe_3O_4). The scheme and description of the preparation of sodium alginate membranes filled with iron oxide nanoparticles is described in Ref. [14].

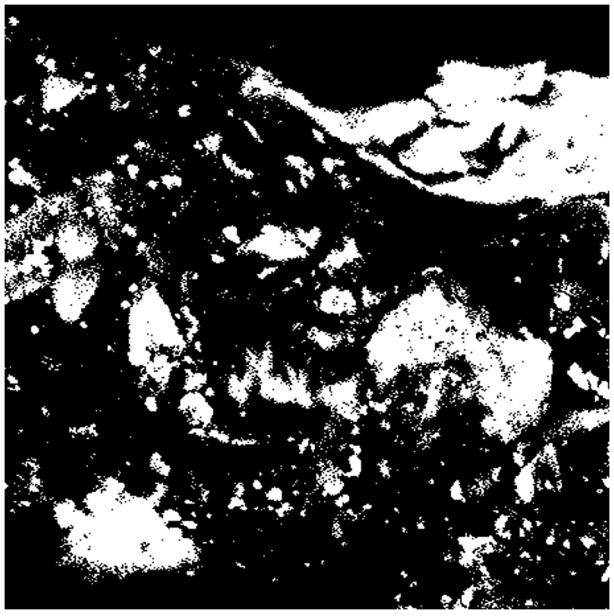

Fig. 1. Model real membrane with magnetic powder. The cross-section of alginate membrane cross-linked by glutaraldehyde containing 25 wt% magnetite particles, magnification 5700×.

The image of the membrane texture was acquired using optical microscopy magnification 5700× and saved as PNG format, which displayed its true colours.

Next, the obtained image was transferred to a black-white format (Fig. 1).

3. Structures of model membranes

Prototype structure, also called model structure, is a useful research tool. It facilitates the development of new research methodologies, their assessment and understanding. This concept is based on the learning procedures, which are often employed in neural networks [20]. In the case of both prototype structures and neural networks, the system and its user must learn how to find a way to display various unique features of a given system.

These features are described by means of quantitative measures. Moreover, essential determination of type and magnitude of changes is important to detect, as well as which features of a selected quantitative measure is sensitive.

This enables researchers to control the creation of a system that can translate desirable properties into the constructed structure [21,22]. Investigations of the model structure's features limit the number of necessary experimental tests. Inevitably, this saves considerable time necessary for performing said experiments, which reduces the overall cost. This work aims to create prototype structures of polymeric membranes with the desired quantity, size and distribution of obstacles (which corresponds to the given amount of filler in the real membrane). The following section describes two algorithms used to generate prototype membranes.

3.1. Algorithms

The membrane is represented by a black and white image where the black regions are available for diffusive particles and the white ones are obstacles, which cannot be penetrated by these tracers. Herein, we used two different methods to generate random artificial membranes of a given density of obstacles. The first method (algorithm A) subdivided the whole membrane into multiple square blocks, each of size $z \times z$ pixels. Each block can independently become an obstacle with probability equal to the given ratio of obstacles. To generate a membrane the following steps are used:

-divide the image into square blocks built of $z \times z$ pixels;
-for each block select a random number from an uniform distribution $U(0, 1)$.
-if the random number for a given block is smaller than the desired ratio of obstacles ρ, all pixels in the block becomes white, otherwise they remains black;

Although the membranes obtained by these approach possesses the desired ratio of obstacles, due to fixed size of the atomic obstacle they are dissimilar to real membranes. Therefore, the second method (algorithm B) accounts for the possibility of irregular, differently shaped obstacles. They are grown around randomly distributed seeds until their desired density ρ is reached. The algorithm is described by the following iterative scheme:

-a black pixel is selected randomly from the image, and a random number ξ is selected from a uniform distribution $U(0, 1)$;
-if $(\xi + p)\cdot(n + 1) > 1.0$, where n is the number of white neighbors of the selected pixel, the pixel becomes white, otherwise it remains black.

In this case the probability that a pixel form obstacle depends on the number of neighbouring white pixels, thus it is more probable that the next white pixel attaches to one of existing obstacles rather than generating a new one. The number and shape of obstacles are indirectly controlled by parameter p. If p value is relatively large, the number of white obstacle seeds at the beginning of generation is high, which will promote a larger number of smaller obstacles. In contrast, smaller p values less obstacles are produced, but their size is larger.

3.2. Generated structures

Using algorithm A, prototype structures (image size:1024 x 1024 pixels) were generated. They had the following parameters:

-colour saturation ratio ρ: 0.25; 0.35; 0.45; 0.50; 0.55; 0.65 and 0.75 (the predicted ratio of the number of filler particles to the size of polymer matrix, which is reflected by the relation of white pixels to black pixels in the image)
-control parameter z: 2, 4, 5, 8, 10, 16, 20, 25, 32, 50, 64, 75, 100, 125, 128, 150 (the parameter defining the size of a basic square obstacle, e.g. 10 signifies a square obstacle of the size 10x10).

Colour saturation ratio corresponds to the number of filler particles added to the polymeric matrix. Filler particles constitute obstacles whose size is defined by the second parameter.

Examples of structures are presented in Fig. 2. In order to precisely describe the obtained textures, the following parameters were calculated for all created structures:

(i)observed amount of polymer matrix ρ,
(ii)fractal dimension of polymer matrix d_f,
(iii)average size of polymer matrix domains S,
(iv)average number of obstacles (white pixels) in the proximity of each polymer matrix pixel n.

Images of artificial membranes generated by algorithm A where z equals 32, 64, 75, and 80 are presented in the Fig. 2. Images of artificial membranes generated by algorithm B where p equals , and $5{\cdot}10^{-6}$ are

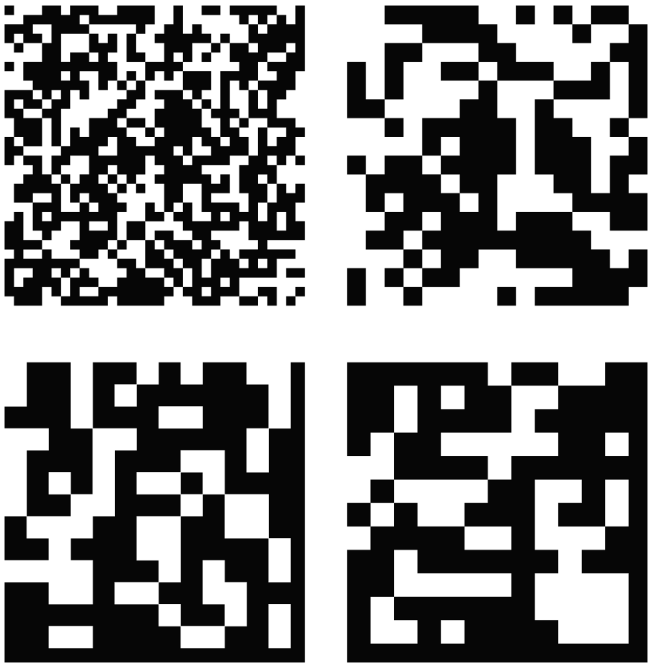

Fig. 2. Images of artificial membranes generated by algorithm A where z equals 32, 64, 75, and 80.

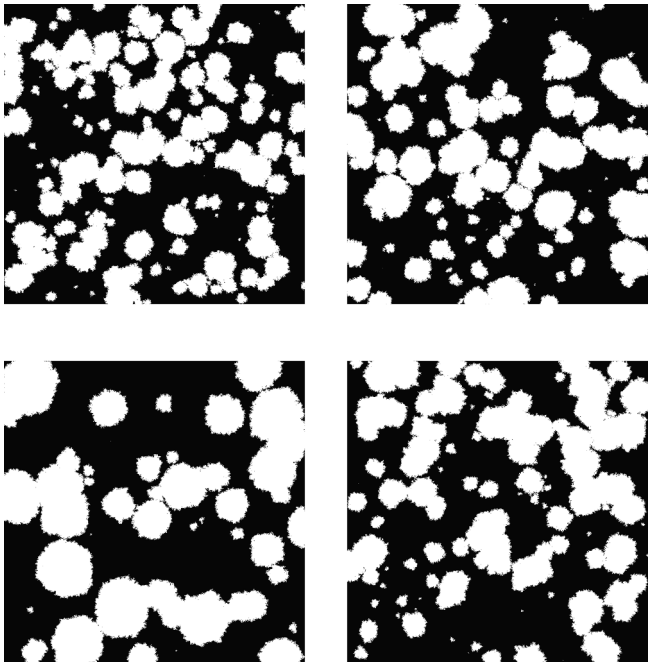

Fig. 3. Images of artificial membranes generated by algorithm B where p equals 10^{-5}, $5{\cdot}10^{-5}$, 10^{-6}, and $5{\cdot}10^{-6}$.

presented in the Fig. 3.

4. Methods

The morphological properties of the studied membranes were quantified using fractal analysis, while transport through the membranes were analysed in terms of Brownian diffusion.

4.1. Morphological analysis

In order to describe quantitatively the morphology of the given real membrane, the digitized image is characterized using the following parameters:

-observed amount of polymer matrix ρ, which is defined as the ratio of the polymer matrix area visible in the picture (black regions) to the total image area,
-fractal dimension of polymer matrix d_f,
-average size of polymer matrix domains S,
-average number of obstacles (white pixels) in the proximity of each polymer matrix pixel n,
-the degree of multifractality ΔD.

Fractal analysis based on fractal dimension d_f and generalized fractal dimension D_q is a practical tool for quantifying the structure and morphology of self-similar objects or structures [14,23,24]. The most common method for calculating fractal dimension is the box counting method. For self-similar sets the number of nonempty coverings $N(\epsilon)$ scales with the current size of covering ϵ in the following way:

$$N(\epsilon) \propto \epsilon^{-d_f} \tag{1}$$

Evaluating the logarithm at the limit $\epsilon \to 0$ results in

$$d_f = \lim_{\epsilon \to 0} \frac{\ln N(\epsilon)}{\ln 1/\epsilon}, \tag{2}$$

where $N(\epsilon)$ is the number of nonempty boxes needed to cover the set, and ϵ is the current size of the box.

Generalized fractal dimension is introduced by means of the

following formula:

$$D_q = \frac{1}{q-1}\lim_{\epsilon\to 0}\frac{\ln\sum_{i=1}^{N(\epsilon)} P_i^q}{\ln \epsilon}, \tag{3}$$

where q is the dimension index, and P_i is the probability of finding a point in a given elements of covering.

The degree of multifractality ΔD is related to the deviation from simple self similarity and constitutes the difference between the maximum and minimum dimension associated with the least dense and most dense points in the sets, as shown in the following formula:

$$\Delta D = D_{-\infty} - D_{+\infty}. \tag{4}$$

4.2. Diffusion on membranes

Properties of diffusive motion on the membranes were studied numerically using their pictures. It was assumed that a single diffusing particle may penetrate the dark regions only and cannot jump over the white areas. The trajectory of such particle was modelled as a set of subsequent random steps. The i-th step is a vector $[dx_i, dy_i]$ was determined using two random variables r_i and ϕ_i:

$$dx_i = r_i\cos\phi_i, \tag{5}$$

$$dy_i = r_i\sin\phi_i, \tag{6}$$

where r_i is drawn from normal distribution $N(0, \sigma)$ and ϕ_i, and ϕ is uniformly distributed on the interval $[0, 2\pi)$. Here, $\sigma = 0.5$ pixels. If the new position of the particle were on a black region it was accepted, and the particle did not cross any white pixels, the move was accepted. Otherwise, it was assumed that the particle reflects from the obstacle and returns to its previous position ($dx_i = 0$ and $dy_i = 0$).

To study diffusion the mean square displacement dependence on the number of trajectory steps were measured and fitted to the relation

$$\langle x^2\rangle = Dt^{\alpha}, \tag{7}$$

where x^2 is the distance from initial to actual position of the particle and t is the number of steps. The averaging was over 10^4 independent trajectories started from random black pixel of a membrane. Parameters D and α are the diffusion constant and the exponent determining character of the diffusion, which equals 1 for standard Brownian motion, and they were fitted from numerical data.

5. Results and discussion

First, the properties of the real membrane (see Fig. 1) were determined. Its morphological properties are characterized by fractal dimension $d_f = 1.9504$, average size of polymer matrix domains $S = 760084$ and the degree of multifractality $\Delta D = 1.5371$. The transport through the membrane is slightly sub-diffusive $\alpha = 0.9362$ and the diffusion constant is $D = 0.00073$.

Using algorithm A, 112 various structures were created (having 7 different values ρ and each having 16 different values of parameter z). An examination on how color saturation ratio and control parameter z (grain size) influence selected structure parameters was conducted, analyzing average size of the domain, fractal dimension and number of neighboring white pixels.

It was ascertained that independently of the selected value of control parameter z, an average size of the domain increases with increasing area occupied by the polymer matrix. This is due to the fusion of smaller domains (Fig. 4). Moreover, when the ratio of obstacles ρ value is close to 0.5 (0.45, 0.5 and 0.55), an increase in domain size occurs parallel to control parameter z.

Fractal dimension depends on both the ρ and z value. It is observed that the value increases with increasing z value above 40, which is due to the fractal dimension that scales the mass of an object. The more the polymer matrix and the less the powder there are, the higher value of the fractal dimension for the generated structure is observed. Fig. 5 shows the correlation between d_f and parameter z as the function having a minimum. For each value of ρ one can find such a value of parameter z that the obtained structure will have the lowest value of fractal dimension. The control parameter z enables the creation of structures with different kinds of self-similarity.

An average number of neighbouring white pixels differentiates structures only in the case when control parameter z has values below 20. When parameter z is higher than 20, an average number of neighbouring white pixels is above 3.9 and asymptotically reaches 4 (Fig. 6).

Using algorithm B, 42 different structures were created (having 7

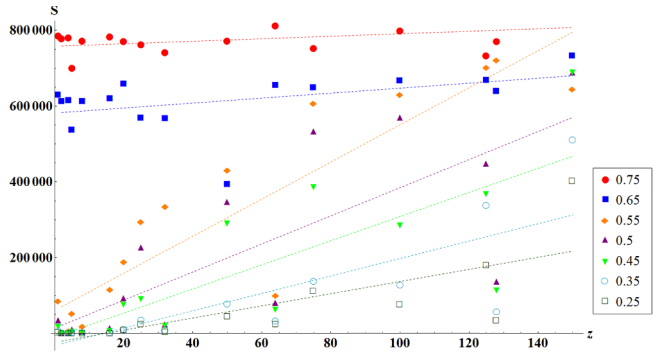

Fig. 4. Dependence between average size of domain S and control parameter z, with changing value of ρ (in the legend).

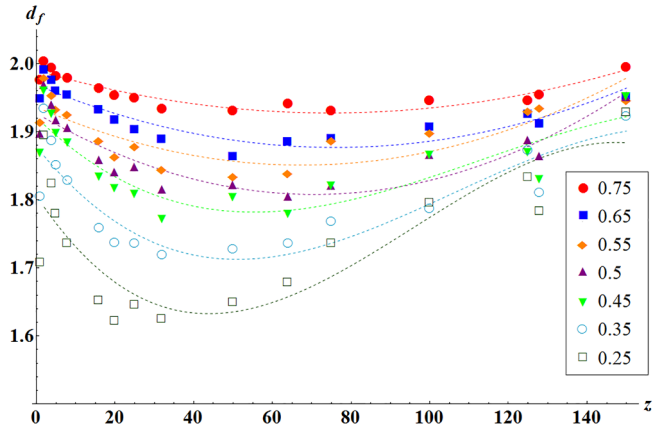

Fig. 5. Dependence between fractal dimension d_f and control parameter z, with changing value of ρ (in the legend).

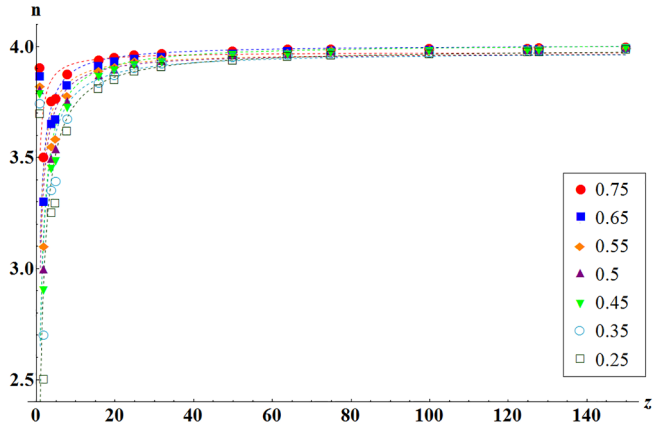

Fig. 6. Dependence between average number of obstacles n and control parameter z with changing value of ρ (in the legend).

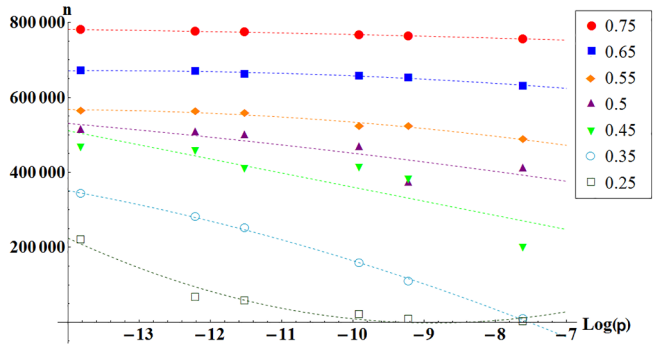

Fig. 7. Dependence between average size of a domain S and control parameter p (which is connected with probability), with changing value of ρ (in the legend).

different ρ values and each possessing 6 different values of parameter p). Analysis of how colour saturation ratio and control parameter p (which is connected with probability) influence selected structure parameters, such as average domain size, fractal dimension and number of neighbouring white pixels is performed. It was ascertained that independently of the selected value of control parameter p (similar to the results from algorithm A), an average size of the domain increases along with the increase of the area occupied by the polymer matrix. It is connected with the fusion of smaller domains (Fig. 7).

The fractal dimension increases with increasing control parameter p (Fig. 8). In contrast, the number of neighbors decreases as the p value increases (Fig. 9).

Results from fractal and morphology analysis of the real membrane and several generated structures are presented in Table 1. The accumulated data in Table 1 and Fig. 10 suggest that structures of artificial membranes generated by algorithm A with parameter $z = 25$ and algorithm B with parameter $p = 10^{-5}$ are comparable to the real membrane structure. Fig. 11 shows images of artificial membranes, using the same parameters for algorithm A and B, respectively. In both cases the parameters are the most similar to those of the real membrane depicted in Fig. 1.

Fig. 12 compares the mean square displacement (MSD) for Gauss process for real membrane and two artificial membranes generated by both algorithms with parameters z and p the most similar to those of the real membrane. The chart shows that the results almost overlap, and the slopes for all functions are similar. These results suggest that diffusion for artificial membranes and for the real one is very similar. Value of α for membrane obtained by using algorithm A is equal 0.9281, and diffusion coefficient is $D = 0.00064$. For prototype membrane generated by algorithm B we determined $\alpha = 0.9493$ and $D = 0.00056$. Whereas α for real membrane is 0.9362 and diffusion

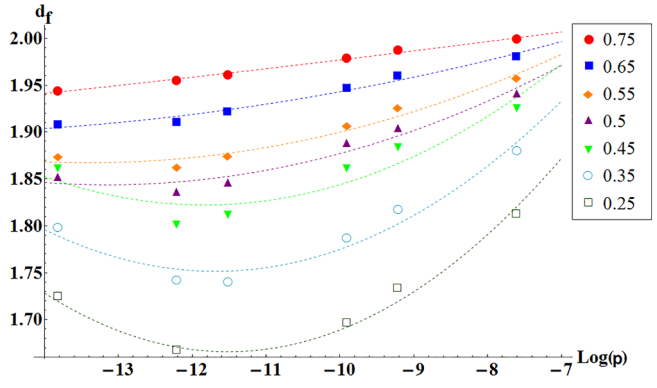

Fig. 8. Dependence between fractal dimension d_f and control parameter p (which is connected with probability), with changing value of ρ (in the legend).

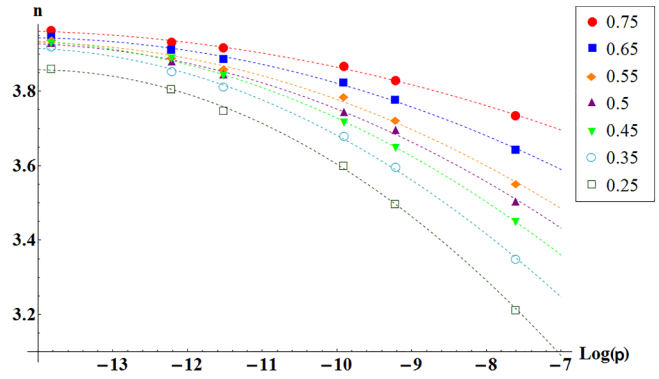

Fig. 9. Dependence between average number of obstacles n and control parameter p (which is connected with probability), with changing value of ρ (in the legend).

Table 1
Results from fractal and morphology analysis for the real membrane and several structures generated by algorithms A and B.

Structure	$1-\rho$	d_F	ΔD	S	n
Real	0.27	1.9504	1.5371	760084.8	3.92
$z = 10$	0.27	1.9708	0.6629	754241.3	3.89
$z = 25$	0.28	1.9458	1.0887	754865.8	3.96
$z = 50$	0.26	1.9300	0.7649	761188.7	3.98
$z = 100$	0.25	1.9453	0.4403	788576.0	3.99
$p = 5{\cdot}10^{-3}$	0.27	2.0067	0.2419	718203.2	3.49
$p = 5{\cdot}10^{-4}$	0.27	1.9958	0.8252	732769.0	3.71
$p = 10^{-4}$	0.27	1.9816	1.2673	741691.7	3.82
$p = 5{\cdot}10^{-5}$	0.27	1.9756	1.2710	746268.0	3.85
$p = 10^{-5}$	0.27	1.9521	1.2740	753207.6	3.91

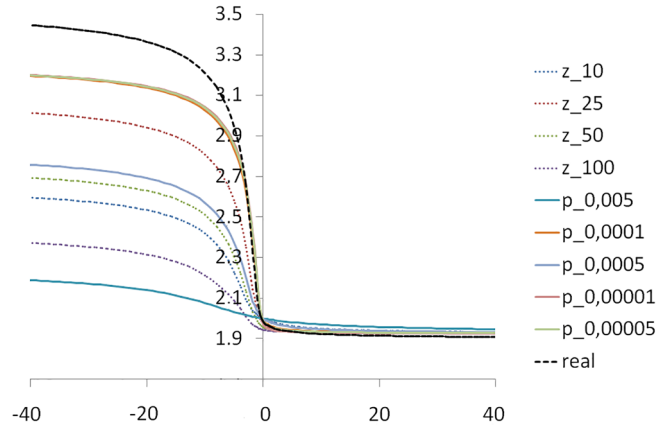

Fig. 10. Spectrum D_q versus q for the real membrane and several structures generated by algorithms A and B.

coefficient is 0.00073. These findings suggest that the generated membranes are very good representation of the real membrane.

6. Conclusions

The main goal of the current study was to generate prototype membrane structures, which resemble real structures. Confirmation of compliance between real and generated membrane structures is possible by examining and comparing structural and transport properties. In the presented studies, the structures of model membranes were generated utilizing a novel program. Two algorithms of structure generation were proposed in order to find the best representation of the real structure. As the first one, Algorithm A was developed, which gave

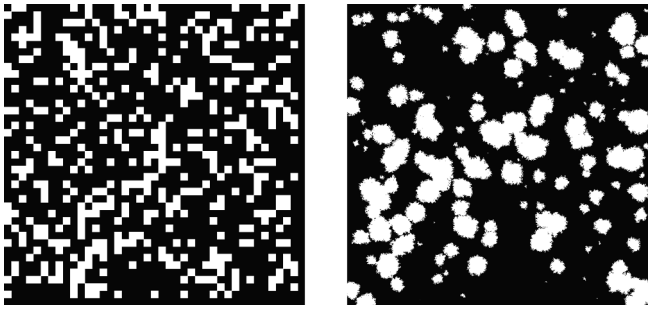

Fig. 11. Images of artificial membranes generated by both algorithms $z = 25$ and $p = 10^{-5}$ with parameters most similar to those of the real membrane form Fig. 1.

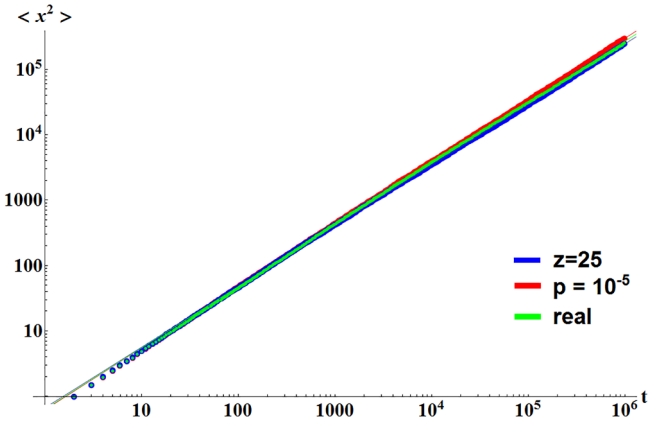

Fig. 12. The dependence of MSD on time for Gauss process for real membrane and two artificial membranes generated by both algorithms with parameters z and p most similar to those of the real membrane.

the possibility to generate the most simplified models of the structure. The whole membrane was subdivided into multiple square blocks. Algorithm B was developed as the second one, which gives the ability to generate more irregular, differently shaped obstacles. Both algorithms A and B enable the generation of prototype structures of preset quantity, size and obstacle distribution. The structures are good models of real-life structures possessing polymer membranes with fillers. The ratio of filling points to the number of matrix points is called ρ parameter and its value is taken from 0.35 to 0.65. Hence, the amount of polymer matrix, which is a space where a particle can move, is between 65% and 35% of the whole area of the picture, respectively. Quantitative description of the membranes morphology is performed using the following parameters: observed amount of polymer matrix ρ, fractal dimension of polymer matrix d_f, average size of polymer matrix domains S and average number of obstacles (white pixels) in the proximity of each polymer matrix pixel n. It has been discovered that the structure formed by the polymer matrix as well as by obstacles was self-similar. The values of calculated fractal dimensions are in the range of 1.83 to 1.96. Correlation between the amount of magnetic powder and the fractal dimensions of the structure of polymer matrix or obstacles is not observed. The fractal structure observed in the images created a complex system, which consists of domains of varied size and shape. The images of artificial membranes generated by algorithms A or B with parameters $z = 25$ and $p = 10^{-5}$, are the most similar to those of the real membrane. The prototype structures with aforementioned parameters became the basis of further research aiming to describe the diffusion on generated structures and compare them with diffusion simulations on real structure. The findings of this investigation complemented those of earlier presented fractal and structure analysis. The most important limitation in current research lies in the fact that magnetite dispersed in alginate membranes is not dispersed uniformly. Sometimes it forms larger aggregations in the membrane in different places, while in other places it is very rare. Such structures are difficult to generate. The present study has been one of the first attempts to thoroughly examine a wide group of alginate membranes with magnetite particles, cross-linked by different agents. Although the current study is described in this paper on a small sample of membrane structures, the presented findings very clearly shows that used algorithms are very useful and give very good results of accordance with real structures. The insights gained from that studies may be of assistance to promote the design of membranes with specific transport properties.

Declaration of Competing Interest

The authors declare that they have no known competing financial interests or personal relationships that could have appeared to influence the work reported in this paper.

Acknowledgement

aaaaaaaaaa

References

[1] N. Fridman-Bishop, V. Freger, What makes aromatic polyamide membranes superior: new insights into ion transport and membrane structure, J. Membr. Sci. 540 (2017) 120–128.
[2] Y. Fan, M. Zhang, R.B. Moore, C.J. Cornelius, Structure, physical properties, and molecule transport of gas, liquid, and ions within a pentablock copolymer, J. Membr. Sci. 464 (2014) 179–187.
[3] G.M. Monsalve-Bravo, S. Smart, S.K. Bhatia, Simulation of multicomponent gas transport through mixed-matrix membranes, J. Membr. Sci. 577 (2019) 219–234.
[4] F. Pan, H. Ding, W. Li, Y. Song, H. Yang, H. Wu, Z. Jiang, B. Wang, X. Cao, Constructing facilitated transport pathway in hybrid membranes by incorporating MoS2 nanosheets, J. Membr. Sci. 545 (2018) 29–37.
[5] G. Enkavi, M. Javanainen, W. Kulig, T. Rag, I. Vattulainen, Multiscale simulations of biological membranes: the challenge to understand biological phenomena in a living substance, Chem. Rev. 119 (2019) 5607–5774 PMID: 30859819.
[6] R. Metzler, J.-H. Jeon, A. Cherstvy, Non-brownian diffusion in lipid membranes: Experiments and simulations, Biochimica Biophys. Acta (BBA) – Biomembranes 1858 (2016) 2451–2467 Biosimulations of lipid membranes coupled to experiments.
[7] R. Zarca, A. Ortiz, D. Gorri, I. Ortiz, Generalized predictive modeling for facilitated transport membranes accounting for fixed and mobile carriers, J. Membr. Sci. 542 (2017) 168–176.
[8] R. Dettori, Q. Yang, W.I. Whiting, Exploration of anion transport in a composite membrane via experimental and theoretical methods, J. Membr. Sci. 563 (2018) 270–276.
[9] M. Minelli, F. Doghieri, K.G. Papadokostaki, J.H. Petropoulos, A fundamental study of the extent of meaningful application of maxwell's and wiener's equations to the permeability of binary composite materials. part i: a numerical computation approach, Chem. Eng. Sci. 104 (2013) 630–637.
[10] J.H. Petropoulos, K.G. Papadokostaki, F. Doghieri, M. Minelli, A fundamental study of the extent of meaningful application of maxwell's and wiener's equations to the permeability of binary composite materials. part iii: Extension of the binary cubes model to 3-phase media, Chem. Eng. Sci. 131 (2015) 360–366.
[11] K.G. Papadokostaki, M. Minelli, F. Doghieri, J.H. Petropoulos, A fundamental study of the extent of meaningful application of maxwell's and wiener's equations to the permeability of binary composite materials. part ii: A useful explicit analytical approach, Chem. Eng. Sci. 131 (2015) 353–359.
[12] R.M. Barrer, J.H. Petropoulos, Diffusion in heterogeneous media: lattices of parallelepipeds in a continuous phase, Br. J. Appl. Phys. 12 (1961) 691.
[13] A. Strzelewicz, Z.J. Grzywna, Studies on the air membrane separation in the presence of a magnetic field, J. Membr. Sci. 294 (2007) 60–67.
[14] G. Dudek, M. Krasowska, R. Turczyn, M. Gnus, A. Strzelewicz, Structure, morphology and separation efficiency of hybrid Alg/Fe3O4 membranes in pervaporative dehydration of ethanol, Sep. Purif. Technol. 182 (2017) 101–109.
[15] G. Dudek, M. Krasowska, R. Turczyn, A. Strzelewicz, D. Djurado, S. Pouget, Clustering analysis for pervaporation performance assessment of alginate hybrid membranes in dehydration of ethanol, Chem. Eng. Res. Des. 144 (2019) 483–493.
[16] A. Strzelewicz, M. Krasowska, G. Dudek, A. Rybak, R. Turczyn, M. Cieśla, Anomalous diffusion on fractal structure of magnetic membranes, Acta Phys. Pol. B

44 (2013) 955–965.
[17] M. Krasowska, A. Strzelewicz, A. Rybak, G. Dudek, M. Cieśla, Structure and transport properties of ethylcellulose membranes with different types and granulation of magnetic powder, Physica A 452 (2016) 241–250.
[18] M. Krasowska, A. Strzelewicz, G. Dudek, M. Cieśla, Structure-diffusion relationship of polymer membranes with different texture, Phys. Rev. E 95 (2017) 012155 .
[19] Z. Grzywna, Scaling in diffusive transport through membranes, Chem. Eng. Sci. 51 (1996) 4115–4125.
[20] J. Hertz, R. Krogh, R. Palmer, Introduction to the Theory of Neuronal Computation, Addison-Wesley Publishing Company, 1991.
[21] Y.W. Kwon, D.H. Allen, R. Talreja, Multiscale Modeling and Simulation of Composite Materials and Structures, Springer, 2008.
[22] H. Altenbach, S. Kruch, Advanced Materials Modelling for Structures, Springer, 2013.
[23] S. Stach, J. Cybo, J. Chmiela, Fracture surface – fractal or multifractal? Mater. Charact. 46 (2001) 163–167 STERMAT 2000: Stereology and Image Analysis in Materials Science.
[24] S. Stach, J. Cybo, Multifractal description of fracture morphology: theoretical basis, Mater. Charact. 51 (2003) 79–86.